Physicochem. Probl. Miner. Process., 61(4), 2025, 205281

http://www.journalssystem.com/ppmp

Physicochemical Problems of Mineral Processing

ISSN 1643-1049

A study on the mechanism of flotation separation between chalcopyrite and sphalerite using Al^{3+} and Tamarind polysaccharide gum as a combined depressant

Tichen Wang [1,2], Jiushuai Deng [1,2], Yijun Cao [3,4], Zhongyi Bai [1,2], Dingquan Xing [1,2]

[1] Inner Mongolia Research Institute of CUMTB, Key Laboratory of Separation and Processing of Symbiotic-Associated Mineral Resources in Non-ferrous Metal Industry, Engineering Technology Research Center for Comprehensive Utilization of Rare Earth - Rare Metal - Rare Scattered in Non-ferrous Metal Industry, School of Chemical & Environmental Engineering, China University of Mining & Technology (Beijing), Beijing 100083, China

[2] National Engineering Laboratory for Efficient Utilization of Indium and Tin Resources, Wuzhou Huaxi Environmental Technology Co., Ltd., Wuzhou 543199, China

[3] Zhongyuan Critical Metal Laboratory, Zhengzhou University, Zhengzhou 450001, China

[4] School of Materials Science and Engineering, Henan University of Science and Technology, Luoyang 471000, China

Corresponding authors: dengshuai689@163.com (Jiushuai Deng), yijuncao@126.com (Yijun Cao)

Abstract: This paper establishes the connection between the characteristics and selectivity behavior of scaly graphite deposits, ores, and minerals from a genetic perspective, and predicts the process indicators. This study explores the relationship between the genetic characteristics of flaky graphite deposits and their mineral processing behavior. Samples from 8 graphite-producing areas in the Jiamusi-Xingkai graphite metallogenic belt were analyzed with the aim of predicting key technological indexes. First, systematic process mineralogy research was carried out. The structural characteristics, chemical composition, mineral composition and particle size distribution, graphite monomer liberation degree, graphite flake size and gangue mineral inclusion between graphite layers were analyzed in detail using techniques such as electron microscopy, the automated quantitative mineral analysis system (MLA), scanning electron microscopy, and the alkali fusion method for graphite flake size determination. In combination with data on ore deposit genesis, beneficiation tests, and production practices, a comparative analysis was performed to identify the genetic characteristics that affect graphite selectivity. These include the degree of metamorphism of the ore deposit, the weathering degree of the ore, the particle size distribution of graphite, and the intergrowth relationships between graphite and typical minerals (such as those prone to slimes, easy-to-float minerals, and flaky minerals). Additionally, a preliminary prediction of concentrate grade and recovery rate was made, and a set of predictive rules for the process flow was established, which aligns with the actual process parameters.

***Keywords*:** chalcopyrite, sphalerite, Al^{3+}, tamarind polysaccharide gum, flotation separation, depressant

1. Introduction

Copper and zinc are crucial non-ferrous metal resources in modern industry, extensively utilized in construction, military, electronics, transportation and etc. (Liu et al., 2020; Zhu et al., 2022). Chalcopyrite and sphalerite are the main sources of copper and zinc metals. However, they often coexist closely in nature (Cui et al., 2022; Liu et al., 2021). Due to economic and technical considerations for smelting requirements, it is essential to separate chalcopyrite and sphalerite before smelting. Currently, foam flotation stands as the primary method for chalcopyrite and sphalerite separation (Chen et al., 2022; Pashkevich et al., 2025). Under normal circumstances, chalcopyrite exhibits better floatability than sphalerite. Nevertheless, the fluid inclusion of chalcopyrite is easily disrupted during grinding, consequently releasing Cu^{2+} that activates sphalerite and diminishes the floatability difference between chalcopyrite and sphalerite (Lai et al., 2019; Hamilton et al., 2024). This poses a significant challenge in

DOI: 10.37190/ppmp/205281

achieving flotation separation of chalcopyrite and sphalerite prior to smelting. Therefore, it is necessary to add sphalerite depressants in the flotation process (Cheng et al., 2025; Wang et al., 2023).

At present, inorganic depressants such as $ZnSO_4$, $NaHSO_3$ and NaCN are used for selectively depression of sphalerite in production practice (Zhang et al., 2022; Liu et al., 2018). Despite their effective flotation separation performance, these inorganic depressants have certain disadvantages including high toxicity, poor biodegradability and serious environmental pollution, which are harmful to human health and the environment (Yin et al., 2017). In response to the growing demand for environmental protection, environmentally-friendly and efficient organic polymer depressants have garnered considerable attention from researchers (Deng ey al., 2023; Wang et al., 2023). Grape skin extract (GPE), which derived from red grape skins rich in monomeric and polymeric polyphenols, was found to adsorb onto mineral surfaces and enhance their hydrophilicity. Xu et al. observed that GPE exhibited stronger adsorption on sphalerite surfaces compared to chalcopyrite, thereby impeding collector adsorption on sphalerite surface and selectively enhancing its hydrophilicity (Xu et al., 2024). Dithiocarbamate chitosan (DTC-CTS) is a product through the reaction of chitosan and CS_2 under alkaline conditions. Liu et al investigated the depression effect of DTC-CTS on sphalerite in chalcopyrite flotation and found that the selective differential adsorption of DTC-CTS on the sphalerite surface could effectively depress sphalerite (Liu et al., 2021). Fenugreek gum, pectin and locust bean gum are natural organic polymer compounds extracted from plants. Their molecular formula contains numerous hydrophilic groups that can interact with the surface of oxidized sphalerite, thereby depressing the flotation of sphalerite (Wang et al., 2021a; Wang et al., 2022; Feng et al., 2020). Although extensive research has been conducted on natural organic polymer reagents as depressants for sphalerite, there are few reports on the application and mechanism of metal ions and natural organic polymer reagents in the flotation separation of chalcopyrite and sphalerite (Wang et al., 2021b; Feng et al., 2024; Saim et al., 2023).

Tamarind polysaccharide gum (TSG) is a neutral polysaccharide extracted from the endosperm of Tamarind seed, characterized by its non-toxicity, biodegradability, and abundant hydroxyl groups in its molecular structure that facilitate interaction with metal ions on mineral surfaces, making it a potential sphalerite depressant (Sheng et al., 2022; Zhou et al., 2021). It has been reported that the addition of Al^{3+} can improve the selective depression effect of organic depressants such as glucose, water glass and guar gum in flotation separation (Xie et al., 2022; Jin et al., 2023). However, the application of Al^{3+} and TSG as combined depressants in the mineral processing has not been reported.

Therefore, the effects of Al^{3+} and TSG as depressants on the flotation separation of chalcopyrite and sphalerite, as well as the interaction mechanism of Al^{3+} and TSG on sphalerite surface were studied by flotation tests, Zeta potential measurements, adsorption measurements, SEM analyses, solution chemical calculations, XPS analyses. This study could provide reference for promoting the flotation separation of Cu-Zn sulfide ore.

2. Experimental

2.1. Materials and reagents

High-purity bulk samples of chalcopyrite ($CuFeS_2$) and sphalerite (ZnS) were purchased from Yunnan Province, China. Following crushing and screening, the ore samples were hermetically sealed and stored in darkness. Particles size fraction from -74 μm to +38 μm were chosen for flotation and XPS tests, whereas the minerals with particle size (-37 μm) were further ground to -5 um for Zeta potential measurements. The results of X-ray diffraction analysis and chemical analysis for chalcopyrite and sphalerite are shown in Fig. 1 and Table 1, proving that the samples used meet the test requirements.

Tamarind polysaccharide gum was obtained from Shanghai Maclin Co., LTD. The experiment used butyl xanthate (BX), methyl isobutyl carbinol (MIBC) as collector and foaming agent. Sodium hydroxide (NaOH) and hydrochloric acid (HCl) are employed to adjust pH value. All reagents, except for BX and MIBC, were of analytical grade. Deionized water was utilized in all experiments.

2.2. Micro-flotation tests

The flotation test was conducted using the XFG flotation machine equipped with 40 mL flotation cell, and the impeller speed was set to 1600 rpm. The flow chart of the flotation test is illustrated in Fig. 2.

Before each single mineral flotation tests, 2 g mineral samples were ultrasonic treated for 5 min, then added into a flotation cell containing 40 mL deionized water. The pH was adjusted using specific froth

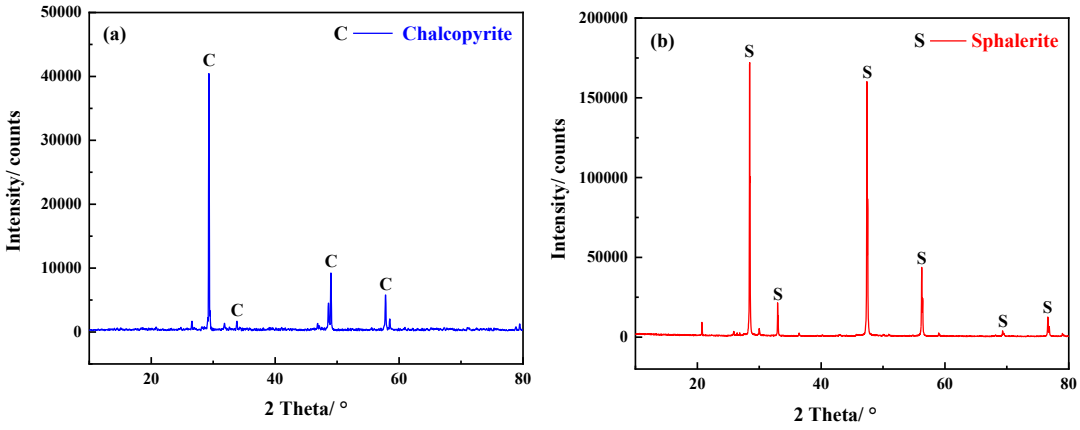

Fig. 1. X-ray diffraction of minerals

Table 1. The chemical composition of chalcopyrite and sphalerite

Mineral	Mass fraction/%			
	Zn	Cu	S	TFe
Chalcopyrite	—	32.19	33.03	29.54
Sphalerite	61.96	—	31.12	1.17

products and tailings were filtered, dried and weighed separately, and the flotation recovery rate concentrations of NaOH and HCl, followed by the addition of specific concentrations of AlCl3, TSG, BX and MIBC in sequence. Then, the froth products were evenly scraped out by hand. Finally, both the was calculated in Eq. 1. For artificial mixed ore tests, the mineral sample consisted of 1.0 g chalcopyrite and 1.0 g sphalerite; following the same procedure as single mineral tests, the flotation recovery rate was calculated in Eq. 2. Each set of flotation tests was repeated at least three times with calculation of their standard deviation.

$$\varepsilon = \frac{m_1}{m_1+m_2} \times 100\% \quad (1)$$

$$\varepsilon = \frac{m_1 \times \alpha_1}{m_1 \times \alpha_1 + m_{2\times} \alpha_2} \times 100\% \quad (2)$$

where ε represents flotation recovery rate(%), m_1 and m_2 represent concentrate and tailings quality respectively, α_1 and α_2 represent concentrate and tailings grade respectively.

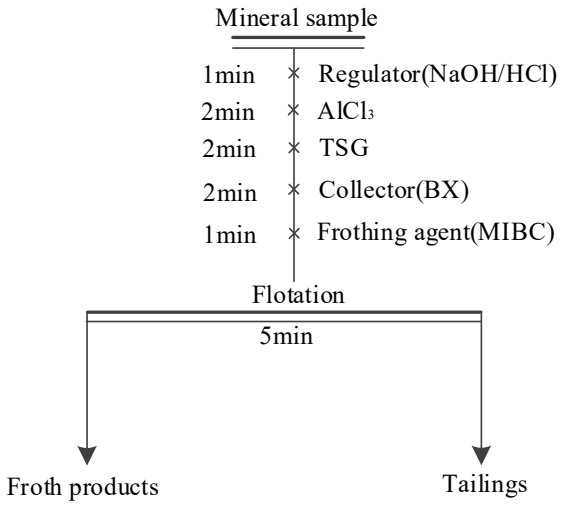

Fig. 2. The flow chart of the flotation test

2.3. Zeta potential measurements

A KNO_3 solution with a concentration of 1×10^{-3} mol/L was prepared in advance. Subsequently, 0.1 g of chalcopyrite or sphalerite samples were dispersed into 40 mL of KNO3 solution and the pH was adjusted to the required value (3, 5, 7, 9, 11) using HCl or NaOH solution. After the addition of the necessary concentration of reagents, the mixture was left to stand for 5 min. The supernatant was taken for zeta potential measurement using Zetasizer (Nano-ZS90, Malvern Instruments Ltd., UK). The tests were repeated three times with same condition and took the average value.

2.4. Adsorption measurements

The UV spectrometer (MAPADA, Japan) was utilized to determine the adsorption density of collector BX on mineral surface. The sample preparation method was as follows: the 2 g mineral sample was placed into a beaker containing 40 mL deionized water, followed by the addition of the necessary concentration of reagents. The reagent was magnetically stirred at a speed of 300 r/min for 30 min. After centrifugal filtration, the filtrate was collected for adsorbance determination. The adsorption capacity of BX on mineral surface is calculated by the residual concentration method, and the specific calculation formula is shown in Eq. 3.

$$\Gamma = \frac{V(C_0 - C_1)}{m} \tag{3}$$

where Γ denotes the adsorption density of BX, C_0 and C_1 are the initial and residual concentration of BX, V represents the volume of solution, m indicates the mass of mineral sample.

2.5. SEM analyses

Surface morphology of chalcopyrite and sphalerite samples was analyzed using scanning electron microscopy (SEM) and Tescan MIRA LMS under various conditions, while the atomic distribution on the surface was determined by energy dispersive spectrometer (EDS).
Solution chemical calculations
Visual MINTEQ software was utilized to predict the potential species and their concentrations in the solution upon addition of 10 mg/L AlCl3. The temperature was set at 25°C, and the pH range was set from 2 to 14. The logarithm of the calculated results was taken to draw the relationship curve between each species' concentration and pH in the solution system. Based on the model data in Visual MINTEQ software, the relationship curve between saturation index (SI) and pH value of precipitation in the solution system is established.

2.6. XPS analyses

XPS is a surface analysis technique used to analyze the chemical environment of surface elements. The surface properties of chalcopyrite and sphalerite were studied by XPS measurements using a K-Alpha spectrometer (Thermo Scientific, USA). All spectra were calibrated using C1s at 284.80 eV. The preparation method of XPS sample is as follows: 2.0 g chalcopyrite or sphalerite was mixed with 40 mL deionized water, after ultrasonic treatment, the reagents of required concentration were added successively, 20 min for stirring, and the sample was filtered and dried in a vacuum drying oven for 6 h.

3. Result and discussion

3.1. Micro-flotation tests

3.1.1. Single mineral flotation

The effects of the dosage of TSG and Al^{3+} on the flotation separation of chalcopyrite and sphalerite using butyl xanthate as a collector was investigated through flotation tests. The test results are presented in Fig. 3. As illustrated in Fig. 3(a), when the concentration of Al^{3+} increased to 20 mg/L, the recovery of chalcopyrite remained relatively stable, while that of sphalerite decreased significantly. The recoveries of both chalcopyrite and sphalerite decreased with the increasing concentration of Al^{3+}, suggesting that the addition of an appropriate concentration of Al^{3+} can widen the difference in floatability between

chalcopyrite and sphalerite. It can be seen from Fig. 3(b) that the recovery of sphalerite gradually decreased with increasing TSG dosage in the absence of Al^{3+}, while the recovery of chalcopyrite remained relatively unchanged. At a TSG concentration of 40 mg/L, there was a 46.67% difference in recovery between chalcopyrite and sphalerite. These results indicated that TSG was a potential sphalerite depressant, which could be utilized in the flotation separation process for chalcopyrite and sphalerite.

With the addition of 10 mg/L Al^{3+}, the recovery of sphalerite gradually decreased with increasing TSG dosage, while the recovery of chalcopyrite remained relatively unchanged. When the Al^{3+} dosage was 10 mg/L and the TSG dosage was 30 mg/L, the difference in recovery between chalcopyrite and sphalerite reached the maximum at 69.39%. These results indicated that the addition of Al^{3+} could enhance the flotation separation of chalcopyrite and sphalerite.

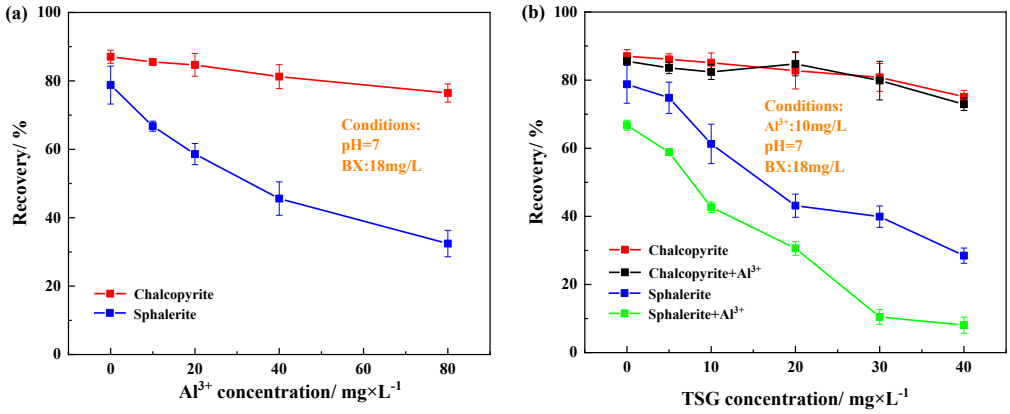

Fig. 3. Effect of Al^{3+} and TSG dosage on the recovery of chalcopyrite and sphalerite

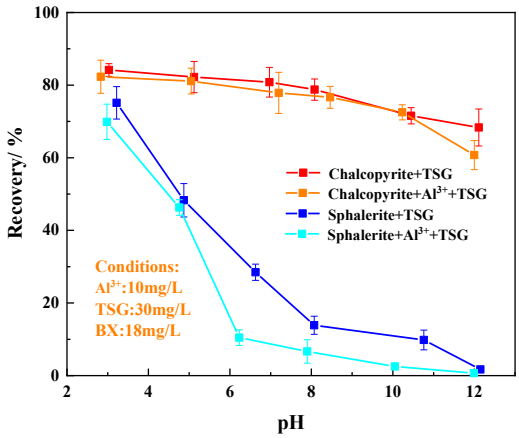

Fig. 4. Effect of pH on the recovery of chalcopyrite and sphalerite treated with different reagents

Fig. 4 illustrates the effect of pH on the recovery of chalcopyrite and sphalerite treated with Al^{3+} and TSG. With the addition of 30mg/L TSG, the recovery of chalcopyrite remained unchanged while that of sphalerite gradually decreased as the pH increased from 3 to 7. When pH increased from 7 to 12, both of chalcopyrite and sphalerite would be depressed, which was not conducive to the recovery of chalcopyrite. Therefore, the optimal pH for flotation separation of chalcopyrite and sphalerite is 7. However, the recovery of sphalerite remained at 27.97% even at pH 7, indicating TSG incompletely depressed sphalerite. With the addition of 10 mg/L Al^{3+} and 30 mg/L TSG, the overall trend was similar to that treated with 30 mg/L TSG. However, the recovery of sphalerite decreased to only 10.48%, while the recovery of chalcopyrite maintained at 79.87% under the tested pH conditions. These results suggested that Al^{3+} together with TSG could achieve the effective separation of chalcopyrite and sphalerite.

3.1.2. Artificial mixed minerals flotation

In order to investigate the effect of Al^{3+} and TSG as depressant on the flotation separation of chalcopyrite and sphalerite, the flotation test of artificial mixed minerals was conducted under the condition of pH=7 and BX concentration of 18 mg/L. As presented in Table 2, the recovery of chalcopyrite and sphalerite in concentrate were more than 70% when BX was used alone, indicating that it was challenging to separate chalcopyrite and sphalerite without depressant. Although the addition of 40 mg/L TSG could selectively reduce the floatability of sphalerite, the recovery of sphalerite remained 36.61%, illustrating that sphalerite was not completely depressed. The flotation separation effect improved when 20 mg/L Al^{3+} and 40 mg/L TSG were added, the recovery of chalcopyrite and sphalerite are 80.63% and 10.07%, respectively. Therefore, Al^{3+} together with TSG will be a promising depressant for the separation of chalcopyrite and sphalerite.

Table 2. The flotation results of artificial mixed minerals

Reagent system	Products	Yield/%	Grade/%		Recovery/%	
			Cu	Zn	Cu	Zn
BX:18mg/L	Concentrate	81.95	16.89	29.52	84.31	73.97
	Tailing	18.05	14.27	47.17	15.69	26.03
TSG:40mg/L,	Concentrate	62.05	22.02	18.73	81.52	36.61
BX:18mg/L	Tailing	37.95	8.16	53.02	18.48	63.39
$AlCl_3$: 20mg/L, TSG: 40mg/L,	Concentrate	45.61	29.38	7.24	80.63	10.07
BX: 18mg/L	Tailing	54.39	5.92	54.25	19.37	89.93

3.2. Zeta potential measurements

Zeta potential is an important parameter of charged properties of mineral surfaces in various systems. The variation of Zeta potential is associated with the adsorption behavior of chemical reagents on mineral surface (Wang et al., 2021). In order to investigate the adsorption behavior of Al^{3+} and TSG on the surface of chalcopyrite and sphalerite, the Zeta potential of chalcopyrite and sphalerite was measured in this study.

It can be seen from Fig. 5 that the Zeta potentials of untreated chalcopyrite and sphalerite decreased with increasing pH, which is consistent with previous findings (Xu et al., 2024). After TSG treatment, the Zeta potential of chalcopyrite had hardly no change at different pH, while the Zeta potential of sphalerite under alkaline condition was obviously shifted positively, indicating that TSG adsorbed on the sphalerite surface.

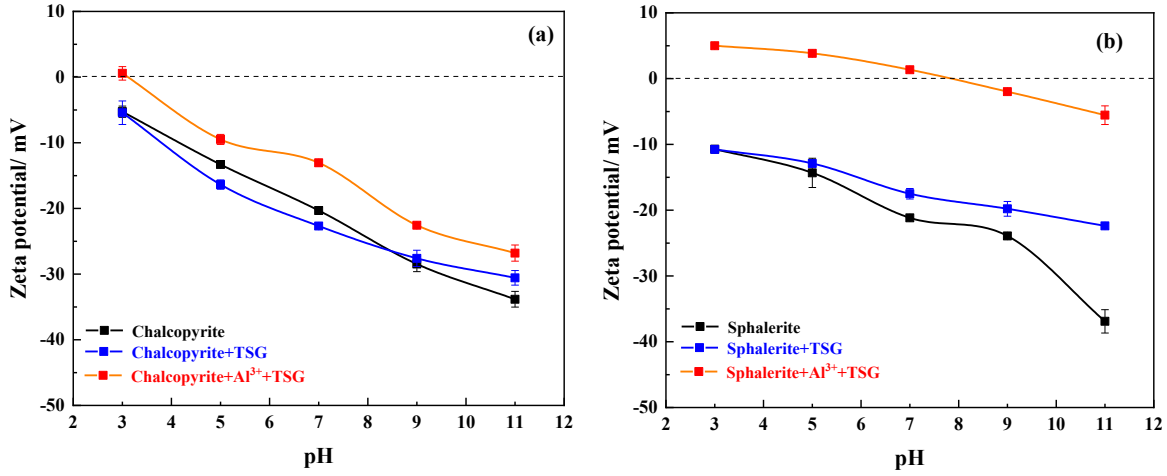

Fig. 5. Zeta potentials of chalcopyrite (a) and sphalerite (b) under different reagents systems

After sphalerite was conditioned with Al^{3+} and TSG, the Zeta potentials of sphalerite significantly shifted toward the positive direction whereas those of chalcopyrite had slightly changed. Moreover, the Zeta potential difference of sphalerite in the presence of Al^{3+} and TSG was larger than that in the

presence of TSG. This phenomenon could be attributed to the ability of positively charged Al^{3+} to mitigate electrostatic repulsion between negatively charged sphalerite and TSG molecules, thereby facilitating the adsorption of TSG on sphalerite (Wang et al., 2021). On the other hand, the interaction between Al^{3+} and chalcopyrite was weaker than that between Al^{3+} and sphalerite, which may be due to the Zeta potentials of chalcopyrite is higher than sphalerite. These results indicated that Al^{3+} effectively promoted the TSG adsorption on sphalerite while it has little effect on chalcopyrite.

3.3. Adsorption measurements

The zeta potential results described above indicated that TSG was adsorbed more strongly on sphalerite than on chalcopyrite after the treatment of Al^{3+}. The adsorption of the collector is directly related to the flotation behavior of the mineral and the addition of depressant may hinder the adsorption of collector on mineral surface (Zhang et al., 2021). Herein, adsorption tests were conducted to determine the adsorption density of BX on these two minerals under different reagents systems at pH=7. The results are illustrated in Fig. 6.

Fig. 6 illustrates that the adsorption density of BX on sphalerite decreased with increasing TSG concentration in the absence of Al^{3+}, while that on chalcopyrite remained relatively stable. At a Al^{3+} dosage of 20 mg/L, the adsorption density of BX on sphalerite significantly decreased with increasing TSG concentration, whereas the adsorption density on chalcopyrite slightly decreased. This suggested that Al^{3+} effectively depressed the adsorption of BX on sphalerite, which might be attributed to its role in depressing sphalerite.

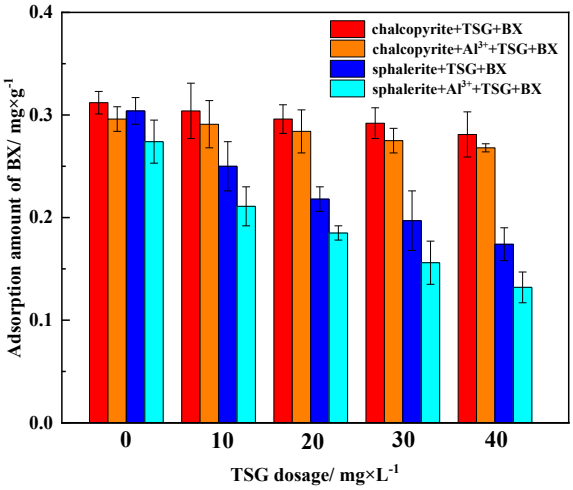

Fig. 6. Effect of TSG dosage on the adsorption density of BX on chalcopyrite and sphalerite with/without the treatment of Al^{3+}

3.4. SEM-EDS analyses

In order to explore the morphological changes of mineral surface, SEM-EDS analyses were conducted on the sphalerite under different conditions. As shown in Fig. 7, the sphalerite treated with TSG exhibited numerous fine granular materials, indicating TSG adsorbed on sphalerite. The result of EDS element mapping revealed a small amount of Al^{3+} on sphalerite after TSG treatment, which probably caused by the Al^{3+} in the environment. Following Al^{3+}/TSG treatment, there was a significant increase in Al content on sphalerite. According to the semi-quantitative results of EDS, the Al content increased from 0.08% to 0.50% and O content increased from 9.84% to 14.46% with the addition of Al^{3+}, suggesting Al^{3+} had the potential to form aluminum oxides.

3.5. Solution chemical calculations

Solution chemistry calculation is a crucial method for understanding the interaction between flotation reagents and mineral surfaces, which also be used to comprehend the dissociation equilibrium of flotation reagents in solution. To further investigate the effect of adding $AlCl_3$ in the solution, Visual

MINTEQ software was utilized to compute the concentration distribution of substances with the addition of 10 mg/L $AlCl_3$ at different pH.

As shown in Fig. 8, Al^{3+} was the predominant component when the pH was below 4. However, the concentrations of $Al(OH)_4^-$ gradually increased as the pH raised. When pH was above 7, $Al(OH)_4^-$ and $Al(OH)_3$ became the predominant components in the solution.

Saturation index (SI) is a parameter that qualitatively predicts the tendency of a component to precipitate or dissolve in solution (Jin et al., 2023). Fig. 9 shows the SI values of potential products in $AlCl_3$ solution at different pH. The SI values of $Al(OH)_3$(s) and Al_2O_3(s) were 5.268 and 4.17 at pH=7 respectively.

Due to precipitation could be formed when SI > 0, the Al_2O_3(s) and $Al(OH)_3$(s) were the possible precipitation species in the solution. The results taken together indicated that aluminum oxides such as

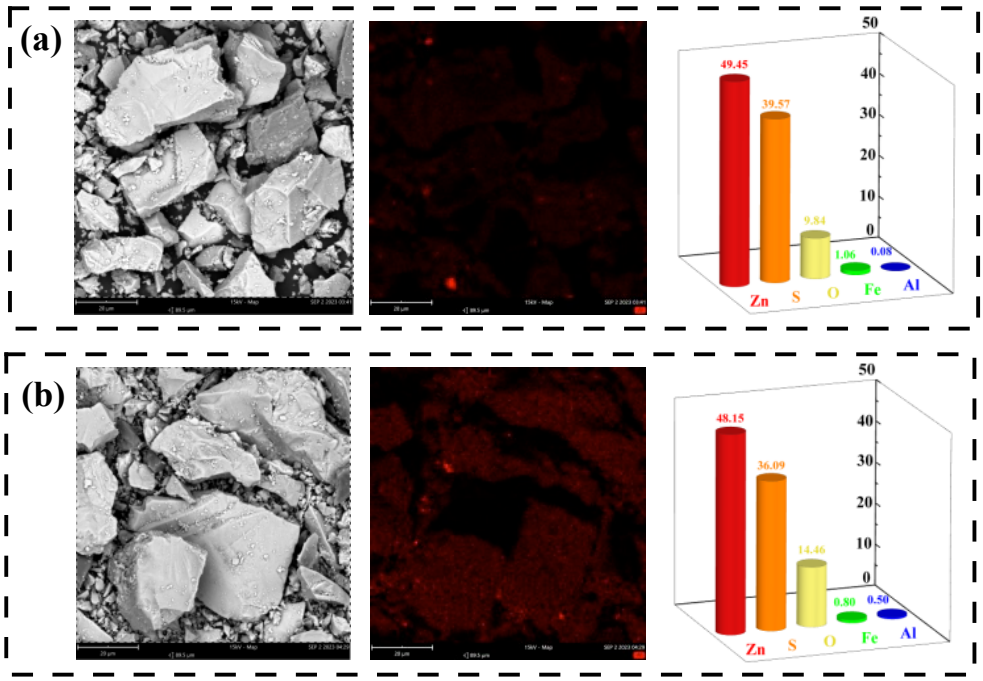

Fig. 7. SEM images, corresponding EDS elemental mapping of Al and the content of EDS spectrum elements for sphalerite after (a) TSG treatment (b) Al^{3+}/TSG treatment

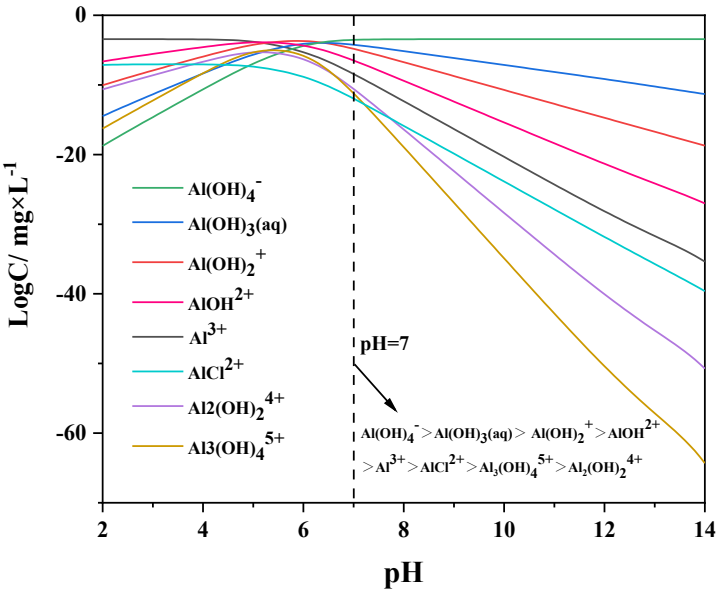

Fig. 8. Graph of the correlation between the concentration of species and pH in 10 mg/L $AlCl_3$ solution

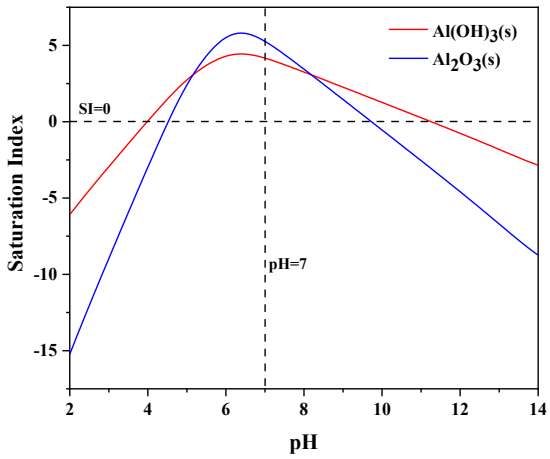

Fig. 9. Graph of the relationship between precipitation SI and pH in 10 mg/L $AlCl_3$ solution

Al_2O_3 and $Al(OH)_3$ (The reactions are shown in Eq. 4-5) might precipitate on sphalerite surface in 10 mg/L $AlCl_3$ solution at pH=7, thereby enhancing the surface hydrophilicity.

$$Al^{3+} + 3Al(OH)_4^- \rightleftharpoons 4Al(OH)_3(s) \quad (4)$$

$$2Al(OH)_3 \rightleftharpoons Al_2O_3(s) + 3H_2O \quad (5)$$

3.6. XPS analyses

In order to further elucidate the adsorption mechanism of Al^{3+} and TSG on sphalerite surface, XPS analyses was conducted on three different sphalerite samples under different conditions. The high-resolution XPS spectra of C 1s, Zn 2p, O 1s and Al 2p of sphalerite samples were plotted, as shown in Fig. 10 and Fig. 11.

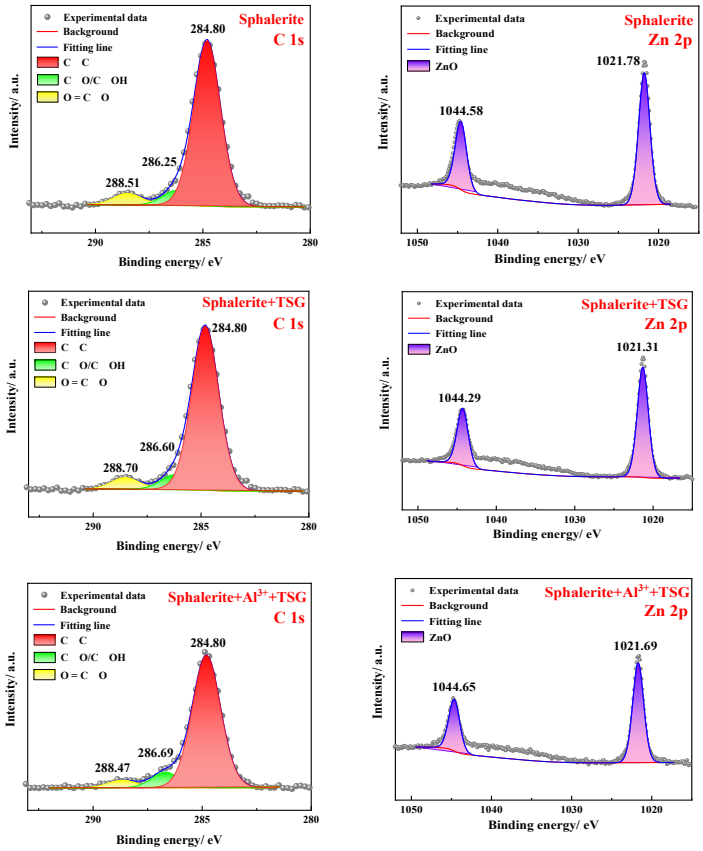

Fig. 10. C1s and Zn2p XPS spectra of sphalerite samples under different conditions

As depicted in Fig. 10, the C 1s peak in the XPS spectrum of untreated sphalerite showed three separated peaks at 284.80, 286.25 and 288.51 eV. These three peaks belonged to C-C, C-O/C-OH and O=C-O, which were attributed to carbon pollution during testing (Xu et al., 2024; Wang et al., 2022). After the addition of TSG, there was a significant shift in the binding energy of the C 1s energy spectrum with an increase of 0.35 eV and 0.19 eV for the peaks ascribed to C-O/C-OH and O=C-O, demonstrating that TSG was attached to the sphalerite surface. After reaction with Al^{3+} and TSG, the C-O/C-OH at 286.60 eV and O=C-O peaks at 288.70 eV shifted by 0.23 eV and 0.09 eV, respectively. The varied binding energy strongly indicated that Al^{3+} might affect the adsorption of TSG on sphalerite. The Zn 2p peak in the XPS spectra of three sphalerite samples under different conditions didn't change significantly, implying that the adsorption of TSG on sphalerite surface may be primarily physical.

Table 3. Atomic ratio analysis of C 1s XPS spectra

Species	Atomic ration/ %		
	C—C	C—O/C—OH	O=C—O
Sphalerite	86.03	7.56	6.41
Sphalerite+TSG	76.96	16.25	6.79
Sphalerite+Al^{3+}+TSG	85.28	9.65	5.07

As depicted in Fig. 11, the O 1s spectrum of pristine sphalerite was fitted with well with two peaks. The two peaks centered at 531.79 and 533.17 eV were associated with C—O and organic oxygen respectively, which was consistent with previous research results (Zeng et al., 2023). After the interaction between sphalerite and TSG, a new significant peak at 532.55 eV was observed, which was attributed to C=O (Deroubaix et al., 2010). The organic oxygen peak at 533.17 eV increased by 0.36 eV, which further confirmed the adsorption of TSG on sphalerite surface (Wang et al., 2021). After the addition of Al^{3+} and TSG, both of the C=O peak and the organic oxygen peak shifted by 0.09 eV. These findings indicate that Al^{3+} might be directly involved in the reaction process of TSG and the sphalerite. Besides, there is no obvious Al2p peak observed in the XPS spectra of sphalerite before treatment with Al^{3+}. However, a new peak at 74.62 eV belonged to $Al(OH)_3$ was observed on sphalerite after treatment with Al^{3+}, demonstrating that the Al^{3+} might be adsorbed on sphalerite by hydrolysis to $Al(OH)_3$ (Rueda et al., 1996).

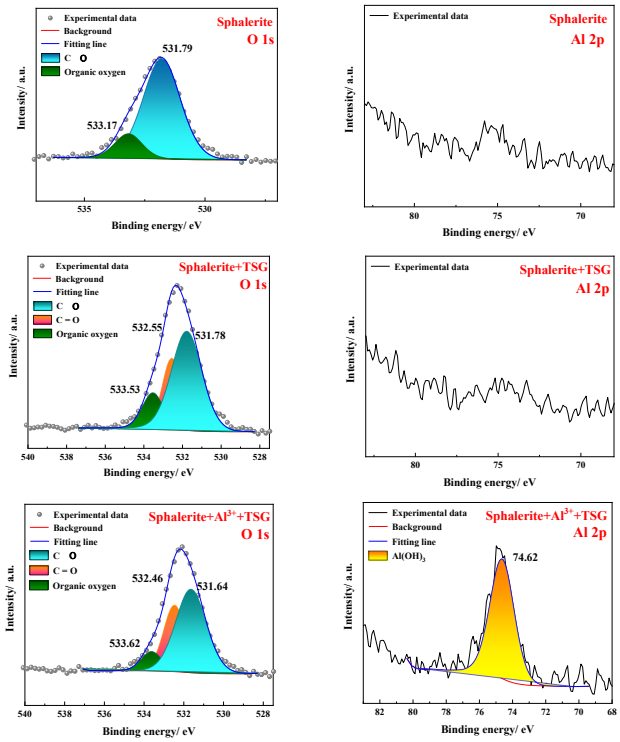

Fig. 11. O 1s and Al 2p XPS spectra of sphalerite samples under different conditions

In order to further study the interaction of Al^{3+} and TSG on sphalerite, the atomic ratios of C 1s and O 1s XPS spectra of sphalerite under different conditions were analyzed (as shown in Table 2 and Table 3). After treatment with TSG, there was a significant alteration in the atomic composition of sphalerite. Specifically, the atomic ratio of C-O/C-OH increased from 7.56% to 16.25%, providing further evidence for the adsorption of TSG on sphalerite (Miao et al., 2022). Interestingly, the atomic ratio of C-O/C-OH decreased by 6.60% after adding Al^{3+}, while the atomic ratio of metal hydroxide increased by 6.56%, indicating Al^{3+} may change the bonding mode between C-O/C-OH in TSG and the sphalerite.

The above results demonstrated that TSG could interact with hydroxylated sphalerite surface by physical adsorption, depressing the flotation of sphalerite. After the addition of Al^{3+}, the hydrophilic $Al(OH)_3$ produced by the hydrolysis of Al^{3+} adsorbed on sphalerite, improving the hydrophilicity of sphalerite and increasing the atomic ratio of metal hydroxide on sphalerite surface. Furthermore, the metal hydroxide on sphalerite surface would provide more adsorption sites for TSG and improved the adsorption density of TSG on sphalerite. Therefore, Al^{3+} together with TSG significantly depressed the flotation of sphalerite.

Table 4. Atomic ratio analysis of O 1s XPS spectra

Species	Atomic ration/%		
	C—O	Organic oxygen	C=O
Sphalerite	85.27	14.73	—
Sphalerite+TSG	58.92	14.50	26.58
Sphalerite+Al^{3+}+TSG	58.02	8.84	33.14

3.7. Depression mechanism

Based on the comprehensive analyses, a potential depression mechanism model of Al^{3+} together with TSG on the flotation of sphalerite is proposed (as shown in Fig. 12), the discussion is presented below:

(1) TSG is a neutral plant gum with strong hydrophilicity which could be adsorbed on sphalerite. The presence of Al^{3+} will reduce the electrostatic repulsion between negatively charged sphalerite and TSG, thereby promoting the adsorption of TSG on sphalerite and improving the hydrophilicity of sphalerite.

(2) Al^{3+} can increase the atomic ratio of metal hydroxide on sphalerite surface, providing more adsorption sites for TSG and enhancing the depression effect of TSG on sphalerite.

(3) $Al(OH)_3$, produced by hydrolysis of Al^{3+}, will adsorb on sphalerite surface and improve its hydrophilicity.

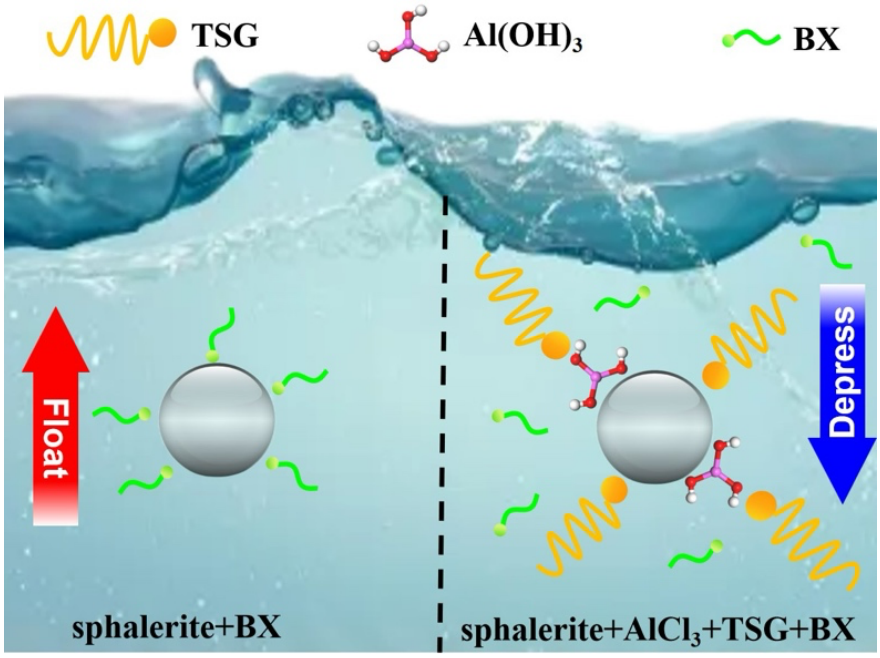

Fig. 12. A potential depression mechanism model of Al^{3+} and TSG on the flotation of sphalerite

4. Conclusion

The effects of Al^{3+} and TSG as depressants on the flotation separation of chalcopyrite and sphalerite, and their depression mechanism were studied using flotation tests, Zeta potential measurements, adsorption measurements, SEM analyses, solution chemical calculations, XPS analyses. The main conclusions are as follows:

(1) TSG could selectively depress sphalerite under neutral or alkaline conditions. The adsorption of TSG on sphalerite surface was stronger than that on chalcopyrite surface.

(2) $Al(OH)_3$ might precipitate on sphalerite surface in Al^{3+} solution, providing additional adsorption sites for TSG and strengthening its depression effect on sphalerite. Besides, the addition of Al^{3+} could enhance the depression effect of TSG on sphalerite.

(3) Al^{3+} and TSG has good prospects to be used as depressants in future to realize the effcient flotation separtion between chalcopyrite and sphalerite.

Acknowledgements

The authors thank the Guangxi Key Technologies R&D Program (Guike AB24010028), Fund Project of State Key Laboratory of Nuclear Resources and Environment (East China University of Technology) (2022NRE-LH-03), Scientific Research Innovation Capability Support Project for Young Faculty (ZYGXONJSKYCXNLZCXM-E3P), 2023 Science and Technology Support Project for the Construction of the Hohhot-Baotou-Ordos National Independent Innovation Demonstration Zone and Major Project of Ordos Iconic Innovation Team (2023XM06/202204) for financial support.

References

CHEN, Y., FENG, B., ZHONG, C., WANG, Z., 2022. *Effect and mechanism of the xanthate/H2O2 addition order on flotation separation of chalcopyrite and sphalerite*. Minerals Engineering. 188, 107851.

CHENG, T., WANG, T., SHEN, Z., MA, S., SHI, S, DENG, J., DENG, J., 2025. *The depression mechanism of magnesium on the flotation of sphalerite with different iron contents: DFT and experimental studies*. Separation and Purification Technology. 353.

CUI, Y., JIAO, F., QIN, W., WANG, C., LI, X., 2022. *Flotation separation of sphalerite from galena using eco-friendly and efficient depressant pullulan*. Separation and Purification Technology. 295.

DENG, J., YAO, W., LIN, Y., QIN, Q., HU, T., XING, J., 2023. *Thoughts on the greening of the mining and utilization of metal mineral resources in deep underground/sea/space*. Journal of Green Mine. 1(01), 186-92.

DEROUBAIX, G., MARCUS, P J S., 2010. *X-ray photoelectron spectroscopy analysis of copper and zinc oxides and sulphides*. Surface & Interface Analysis. 18(1), 39-46.

FENG, Y., CHEN, Y., CHEN, J., 2024. *The mechanism of surface activation in sphalerite by metal ions with d10 electronic configurations: Experimental and DFT study*. Applied Surface Science. 649.

FENG, B., ZHONG, C., ZHANG, L., GUO, Y., WANG, T., HUANG, Z., 2020. *Effect of surface oxidation on the depression of sphalerite by locust bean gum*. Minerals Engineering. 146, 106142.

HAMILTON, D., CHANG, W., MCPHEDRAN, K. N., 2024. *Establishing an optimized flotation scheme for a complex Base-Metal sulfide ore using a modified xanthate reagent scheme*. Minerals Engineering. 216.

JIN, D., SUN, R., WANG, G., DENG, J., ZHANG, X., 2023. *Flotation separation of fluorite and calcite using anhydrous glucose and aluminum sulfate as a combined depressant*. Applied Surface Science. 624.

LAI, H., DENG, J., WEN, S., WU, D., 2019. *Homogenization phenomena of surface components of chalcopyrite and sphalerite during grinding processing*. Colloids and Surfaces A: Physicochemical and Engineering Aspects. 578, 123601.

LIU, J., HAO, J., DONG, W., ZENG, Y., 2021. *Depression mechanism of environment-friendly depressant dithiocarbamate chitosan in flotation separation of Cu-Zn sulfide*. Colloids and Surfaces A: Physicochemical and Engineering Aspects. 615.

LIU, J., WANG, Y., LUO, D., ZENG, Y., 2018. *Use of $ZnSO_4$ and SDD mixture as sphalerite depressant in copper flotation*. 121, 31-8.

LIU, D., ZHANG, G., CHEN, Y., HUANG, G., GAO, Y., 2020. *Investigations on the utilization of konjac glucomannan in the flotation separation of chalcopyrite from pyrite*. Minerals Engineering. 145.

MIAO, Y., WEN, S., SHEN, Z., FENG, Q., ZHANG, Q., 2022. *Flotation separation of chalcopyrite from galena using locust bean gum as a selective and eco-friendly depressant*. Separation and Purification Technology. 283.

PASHKEVICH, D., MOHAMMADI-JAM, S., KÖKKILIÇ, O., WATERS, K. E., 2025. *Temperature impact on xanthate adsorption and microflotation of galena, sphalerite, and pyrite.* Chemical Engineering Science. *304.*

RUEDA, F., MENDIALDUA, J., RODRIGUEZ, A., Rodrigo, C., 1996. *Characterization of Venezuelan laterites by X-ray photoelectron spectroscopy*. Journal of Electron Spectroscopy and Related Phenomena. 82(3), 135-43.

SAIM, A. K., DARTEH, F. K., 2023. *Eco-Friendly and Biodegradable Depressants in Chalcopyrite Flotation: A Review*. Mineral Processing And Extractive Metallurgy Review. 44(7), 492-510.

SHENG Q., YIN, W., MA, Y., LIU, Y., WANG, L., YANG, B., SUN, H., YAO, J., 2022. *Selective depression of talc in azurite sulfidization flotation by tamarind polysaccharide gum: Flotation response and adsorption mechanism*. Minerals Engineering. 178.

WANG, C., LIU, R., SUN, W., JING, N., XIE, F., ZHAI, Q., HE, D., 2021. *Selective depressive effect of pectin on sphalerite flotation and its mechanisms of adsorption onto galena and sphalerite surfaces*. Minerals Engineering. 170.

WANG, C., LIU, R., WU, M., ZHAI, Q., SUN, W., JING, N., XIE, F., 2021. *Induced adsorption of pectin on copper-ion-modified galena surfaces: Flotation and adsorption mechanism*. Minerals Engineering. 173.

WANG, C., LIU, R., WU, M., ZHAI, Q., LUO, Y., JING, N., XIE, F., SUN, W., 2022. *Selective separation of chalcopyrite from sphalerite with a novel depressant fenugreek gum: Flotation and adsorption mechanism*. Minerals Engineering. 184.

WANG, T., SUN, G., DENG, J., XU, H., WANG, G., HU, M., QIN Q., SUN, X., 2023. *A depressant for marmatite flotation: Synthesis, characterisation and floatation performance*. International Journal of Minerals, Metallurgy and Materials. 30(6), 1048-56.

WANG, L., DENG, J., WANG, R., 2023. *Evolution and reconstruction of the scientific connotation of green mine*. Journal of Green Mine. 1(01), 178-85.

XIE, X., LI, B., XIE, R., TONG, X., LI, Y., ZHANG, S., LI, J., SONG, Q., 2022. *Al^{3+} enhanced the depressant of guar gum on the flotation separation of smithsonite from calcite*. Journal of Molecular Liquids. 368.

XU, X., ZHANG, X., ZHANG, Y., LIU, X., HE, H., FANG, J., SHEN, P., PENG, R., YU, J., CHEN, X., 2024. *A study on the mechanism of flotation separation between chalcopyrite and sphalerite using a novel environmental depressant derived from grape peel extract GPE*. Colloids and Surfaces A: Physicochemical and Engineering Aspects. 681.

YIN, Z., SUN, W., HU, Y., ZHAI, J., GUAN, Q., 2017. *Evaluation of the replacement of NaCN with depressant mixtures in the separation of copper–molybdenum sulphide ore by flotation*. 173, 9-16.

ZENG, Y., WANG, C., HE, J., HUA, Z., CHENG, K., WU, X., SUN, W., WANG, L., HU, J., TANG, H., 2023. *Selective depressing mechanism of H-acid monosodium salt on flotation separation of graphite and sphalerite*. 33(12), 3812-24.

ZHANG, Y., ZHANG, X., LIU, X., ZHANG, T., NING, S., SHEN, P., LIU, Z., LAI, H., LIU, D., YANG X., 2022. *Carrageenan xanthate as an environmental-friendly depressant in the flotation of Pb–Zn sulfide and its underlying mechanism*. Colloids and Surfaces A: Physicochemical and Engineering Aspects. 653.

ZHANG, S., DENG, Z., XIE, X., TONG, X., 2021. *Study on the depression mechanism of calcium on the flotation of high-iron sphalerite under a high-alkalinity environment*. Minerals Engineering. 160.

ZHU, H., YANG, B., MARTIN, R., ZHANG, H., HE, D., LUO, H., 2022. *Flotation separation of galena from sphalerite using hyaluronic acid (HA) as an environmental-friendly sphalerite depressant*. Minerals Engineering. 187.

ZHOU, H., YANG, Z., TANG, X., SUN, W., GAO, Z., LUO, X., 2021. *Enhancing flotation separation effect of fluorite and calcite with polysaccharide depressant tamarind seed gum*. Colloids and Surfaces A: Physicochemical and Engineering Aspects. 624.